Genome Biology and Evolution Advance Access published July 12, 2016 doi:10.1093/gbe/evw163

Gene expression profiling in the hibernating primate, *Cheirogaleus medius*

Sheena L. Faherty*[1, a], José Luis Villanueva-Cañas[2, a], Peter H. Klopfer[1], M. Mar Albà[2, 3], and Anne D. Yoder[1]

[1] Department of Biology, Duke University, Durham, NC 27708, USA

[2] Evolutionary Genomics Group, Research Programme on Biomedical Informatics (GRIB), Hospital del Mar Research Institute (IMIM), Universitat Pompeu Fabra (UPF), Barcelona, Spain

[3] Catalan Institution for Research and Advanced Studies (ICREA), Barcelona, Spain

[a] Authors contributed equally to this work

*Author for Correspondence: Sheena L. Faherty, Biology Department, Duke University, Durham, NC, USA, Tel: 262-894-0333, E-mail address: sheena.faherty@gmail.com

Running title: Gene expression in a hibernating primate

Abstract

Hibernation is a complex physiological response that some mammalian species employ to evade energetic demands. Previous work in mammalian hibernators suggests that hibernation is activated not by a set of genes unique to hibernators, but by differential expression of genes that are present in all mammals. This question of universal genetic mechanisms requires further investigation and can only be tested through additional investigations of phylogenetically dispersed species. To explore this question, we use RNA-Seq to investigate gene expression dynamics as they relate to the varying physiological states experienced throughout the year in a group of primate hibernators—Madagascar's dwarf lemurs (genus *Cheirogaleus*). In a novel experimental approach, we use longitudinal sampling of biological tissues as a method for capturing gene expression profiles from the same individuals throughout their annual hibernation cycle. We identify 90 candidate genes that have variable expression patterns when comparing two active states (Active 1 and Active 2) to a torpor state. These include genes that are involved in metabolic pathways, feeding behavior, and circadian rhythms, as might be expected to correlate with seasonal physiological state changes. The identified genes appear to be critical for maintaining the health of an animal that undergoes prolonged periods of metabolic depression concurrent with the hibernation phenotype. By focusing on these differentially expressed genes in dwarf lemurs, we compare gene expression patterns in previously studied mammalian hibernators. Additionally, by employing evolutionary rate analysis, we find that hibernation-related genes do not evolve under positive selection in hibernating species relative to non-hibernators.

Keywords: RNA-Seq, differential gene expression, *Cheirogaleus*, dwarf lemurs, white adipose tissue

Introduction

To survive in highly seasonal environments, mammals employ a range of phenotypic and behavioral tactics to cope with fluctuating energetic demands. Hibernation is among the most extreme of these strategies. This seasonally expressed period of heterothermy represents a radical deviation from mammalian homeostasis, involving complex physiological and behavioral changes that conserve up to 90% of the energy required to remain euthermic during the winter (Morin & Storey 2009; Geiser & Heldmaier 1995). Classical hibernation behavior is defined by periods of torpor (i.e. controlled reductions in metabolic rate, body temperature (T_b), and heart rate) and metabolically active periods of rewarming known as interbout arousals (IBAs).

The remarkably widespread phylogenetic diversity of hibernation among mammalian lineages raises the question: "Are there fundamental similarities in the molecular architecture underlying the hibernation phenotype?" (Srere et al. 1992; Carey et al. 2003; Villanueva-Cañas et al. 2014). Hibernators are found in fourteen orders of mammals that range from arctic, temperate, and tropical regions, and represent all three of the deepest branches of the Class Mammalia: Monotremata, Marsupialia, and Placentalia (Srere et al. 1992; Carey et al. 2003; Andrews 2007; Figure 1). The current understanding is that the hibernation phenotype arises due to selective expression of genes that are correlated with orchestrating physiological changes that allow a hibernator to experience recurrent torpor bouts during the winter (Yan 2006; Epperson & Martin 2002; Hampton et al. 2011; Fedorov et al. 2011; Williams 2005; Wilson et al. 1992; Bauer et al. 2001; Buck et al. 2002; Eddy 2004; Eddy et al. 2006; Srere et al. 1992; Seim et al. 2013; Schwartz et al. 2013; Hampton et al. 2013; Lei et al. 2014; Grabek et al. 2015; Vermillion et al. 2015; Epperson et al. 2010; Shao et al. 2010; Suozzi et al. 2009; Emirbekov & Pashaeva 2014;

Mominoki et al. 2005; Mominoki 1998; Chow et al. 2013). However, it is unknown if distantly related species use the same key pathways for activating and maintaining the hibernation phenotype. Our study contributes to a broader sampling across the mammalian phylogeny by incorporating a group of primate hibernators, the dwarf lemurs of Madagascar (genus *Cheirogaleus*), and thus has the potential to provide unique insight into the question of a universal genetic regulatory pathway of hibernation.

Dwarf lemurs belong to one of two clades within the primate lineage to manifest depressed metabolic rates via torpor. The closely related mouse lemurs, which, like dwarf lemurs, are members of the family Cheirogaleidae, are capable of torpor (Ortmann et al. 1997; Schmid 2001), although torpor bouts in these animals are typically shorter than 24 hours. The other primate clade to express torpor is the Lorisiformes. The Asian pygmy slow loris was most recently documented to demonstrate bouts of sustained metabolic suppression under semi-captive conditions (Ruf et al. 2015), while anecdotal reports of torpor have also been reported for their sister lineage, the bushbabies, under extreme energetic demands (e.g. Nowack et al. 2013). In the western regions of Madagascar, fat-tailed dwarf lemurs (*Cheirogaleus medius*) engage in hibernation for up to 7 months wherein body temperature approximates ambient temperature (Dausmann et al. 2004; 2005; 2009). Madagascar is highly seasonal, with severe shortages of rain and associated resources during the winter. In response, fat-tailed dwarf lemurs enter hibernation to reduce energetic costs when dry spells occur (Dausmann et al. 2005; 2004; 2009). When occupying well-insulated hibernacula, fat-tailed dwarf lemurs display a classic hibernation pattern including characteristic IBAs; however, when hibernating in poorly insulated tree holes, they can abandon an active defense of T_b and switch to a poikilothermic state where T_b

thermoconforms to ambient without the demand for IBAs (Dausmann et al. 2004). This is in contrast to every other known hibernating species (except members of the family Ursidae and Tenrecidae; Toien et al. 2011, Lovegrove et al. 2014). Presumably the ability to thermoconform under poorly insulated conditions allows these tropical primates to engage in hibernation, even at widely fluctuating (i.e. oscillations of more than 30 degrees in a single day), elevated T_a (Dausmann et al. 2009; 2005).

Dwarf lemurs can more than double their body weight by building up reserves of white adipose tissue (WAT) preceding hibernation and then use these stores as an energy reservoir during the prolonged period of physical inertia (Fietz & Dausmann 2007). In captivity, even in the absence of environmental triggers such as food scarcity and lowered temperatures, fat-tailed dwarf lemurs nonetheless exhibit seasonal body mass cycles. This seasonal response, irrespective of environmental conditions, strongly suggests that underlying clock-like molecular mechanisms are responsible for seasonal fat deposition (Perret et al. 1998; Perret & Aujard 2001; Dark 2005).

WAT is an especially informative organ for study in the context of the hibernation phenotype given that fat deposition and metabolism are critical aspects of survival during hibernation. Fat-storing hibernators switch their metabolic economy from carbohydrates during the active season, to lipids during the hibernation season as a means to conserve energy (Carey et al. 2003; Boyer & Barnes 1999; Buck et al. 2002). Investigations of how annual body mass cycles are governed by underlying molecular mechanisms in WAT have been conducted in multiple mammalian lineages using candidate gene approaches (Eddy 2004; Herminghuysen et al. 1995; Boyer et al. 1998; Wilson et al. 1992; Demas et al. 2002; Bauer et al. 2001; Kabine et al. 2004; Buck et al.

2002; Eddy et al. 2005), and recently using next-generation sequencing (Hampton et al. 2011) in a subset of mammalian model hibernators. These studies have laid the groundwork for establishing the paradigm that differential gene expression is correlated with physiological changes throughout the year. Though one previous study employed a longitudinal approach to investigate protein levels in the blood serum of black bears (Chow et al. 2013), ours is the first to examine levels of gene expression in biological tissues (i.e., WAT) from the same animals at multiple times points during the year. This is a powerful approach for controlling for inter-individual variation, which might otherwise confound differential gene expression analyses.

It is currently unknown how seasonal body mass cycles are regulated in dwarf lemurs, and if dwarf lemurs conform to the conventional paradigm that changes in metabolic economy occur in conjunction with variations in gene expression throughout the course of the circannual cycle. Therefore, in the present study, we use gene expression data generated from an RNA-Seq experiment, sampled longitudinally in multiple animals, to examine the genetic controls behind the metabolic switch from carbohydrate to lipid metabolism in dwarf lemurs. We compare our results to previously published data from model mammalian species to provide further insight into the question of whether the hibernation phenotype in distantly related mammalian hibernators is controlled by the same regulatory pathways (Villanueva-Cañas et al. 2014).

Materials and Methods

Animals and care regimen. All animals examined in this study were captive born and have been maintained under captive conditions throughout their lifespan. The fat-tailed dwarf lemur colony maintained at the Duke Lemur Center (DLC) offers a unique resource for systematically

sampling key biological tissues under carefully controlled conditions using a longitudinal sampling approach. A total of four (2 male and 2 female) fat-tailed dwarf lemurs were used throughout this study with ages ranging from 8-13 years old. At the beginning of the hibernation season at DLC (November), dwarf lemurs were moved into a specially constructed hibernaculum, which allowed independent control of photoperiod and temperature. Animals were caged separately, but allowed visual and auditory access to other individuals. Individuals were provided water *ad libitum* and a standard DLC diet of Purina primate chow, fruits/vegetables, and mealworms. Under captive conditions, dwarf lemurs are provided multiple nesting tubes to mimic their natural habitat, where they hibernate in tree holes, and are therefore still exposed to photoperiodic triggers. Study animals are exposed to simulated natural conditions, including a 66% reduction in caloric input preceding torpor to simulate reduced food resources, shortened daylight hours, and lowered ambient temperature, so as to induce seasonal torpor during the months of January-February.

Experimental collection points. Three experimental time points were used: October (Active 1), December (Active 2), and February (Torpor) to represent a wide range of physiological changes that coincide with changes in seasonality (Figure 2). Physiological state at each collection point was verified by rectal T_b and body mass was recorded at the time of sampling (Table 1; individual animal's data can be found in Table S1). The only difference between October and December was a gradual decrease in daylight hours from 11.5 hours to 9.5 hours of daylight, simulating the transition from summer into fall. Our initial goal was to compare three distinct physiological states, including a period of extreme fattening during December (Active 2). Due to federally mandated standards, however, animals included in our study were not allowed to feed

ad libitum during the fall months which, in wild populations, is crucial for maximum fat accumulation preceding the hibernation season. This dietary restriction may therefore have had important consequences for the comparison of Active 1 relative to the Active 2 collection points.

During a torpor bout, dwarf lemurs exhibit decreases in T_b to as low as 15°C, reductions in heart rate to 3-5 beats per minute, and episodes of irregular and infrequent breathing (Krystal et al. 2013; Dausmann et al. 2004). We sampled WAT from animals when they were 2-3 days into a torpor bout as determined by an absence of feeding.

Tissue collection. We successfully used minimally invasive sampling techniques to acquire tissue samples of WAT. Animals were anesthetized using Ketamine (10 mg/kg; Ketaject, Bioniche Teoranta; Galway, Ireland) and Midazolam (0.25 mg/kg; Bedford Laboratories; Bedford, OH) by a DLC veterinarian. Sampling procedures took place at a consistent daily time point (between 9:00-10:00 am) to account for any circadian fluctuations influencing gene expression profiles. Tissue samples of WAT were obtained using needle biopsy from the section of the tail where fat storage was most concentrated (Fietz et al. 2003). The area to be sampled was shaved and skin was cleaned with chlorhexidine solution followed by alcohol three alternating times. Skin was held taught and a 16-gauge tru-cut biopsy needle (Jorgenson Laboratories; Loveland, CO) was inserted in target area. Biopsy was removed and tissue sample was expelled directly into RNA stabilization solution (Qiagen; Valencia, CA). Samples were placed in 4°C overnight, and the next morning moved to storage in -20°C until further processing. The 4°C incubation prior to freezing was done to allow cross-comparisons with samples collected from wild individuals for a future investigation.

RNA purification and whole transcriptome amplification. The entire tissue sample (15-20 mg) was used for RNA isolation procedure. All RNA extractions were conducted on the same day after tissue sampling was complete by the lead author (SLF) to minimize inter-sample variability. Total RNA was purified from WAT using an optimized TRIzol protocol in conjunction with the Microarray Tissue Kit (Qiagen; Valencia, CA). Briefly, frozen tissues were homogenized in 500 µl TRI Reagent (Ambion; Grand Island, NY) using a hand-held rotor-stator homogenizer to provide efficient disruption and homogenization of samples. BCP (1-bromo-3-chloropropane) extraction was performed using 50 µl of BCP, followed by centrifugation at 12,000 x g for 15 min at 4° C. Aqueous layer containing total RNA was transferred to a fresh 1.5 ml centrifuge tube and one volume of 70% EtOH was added. The entire sample volume was loaded onto Qiagen RNeasy filter columns and kit protocol was followed according to manufacturer's instructions, including an on-column DN*ase* step to remove any residual contaminating DNA. RNA integrity and concentration was assessed using the Agilent 2100 Bioanalyzer (Santa Clara, CA) at Duke University's Institute for Genome Science and Policy's Microarray Facility. RIN values for our total RNA extractions ranged from 3.5-6.7 and total RNA concentrations ranged from 2-24 ng/µl. WAT has a high lipid content to nuclear content ratio and extracting sufficient total RNA for downstream RNA sequencing is therefore problematic. To that end, we completed a whole transcriptome amplification step on all total RNA extractions prior to Illumina sequencing.

To account for the wide range in extracted RNA concentrations, purified RNA was diluted to 2 ng/µl in a 5 µl total volume and then subjected to whole transcriptome amplification using

NuGEN's Ovation RNA-Seq V2 kit (San Carlos, CA) according to manufacturer's instructions. This kit provides a rapid method for preparing amplified cDNA from total RNA for downstream RNA-Seq applications. It employs a single primer isothermal amplification (SPIA) method to amplify total RNA into double stranded cDNA and depletes rRNA without preselecting mRNA. Amplified cDNA samples were then purified using the MinElute Reaction Cleanup Kit (Qiagen; Valencia, CA) according to manufacturer's protocol. cDNA concentrations post-amplification ranged from 347-461 ng/µl. In a preliminary analysis using unamplified vs. amplified RNA extracted from rat WAT, we have confirmed that whole transcriptome amplification does not introduce significant bias in relative mRNA frequencies (Faherty et al. 2015). Amplified cDNA samples from dwarf lemurs were then sent to Duke University's Genome Sequencing Shared Resource for library preparation and sequencing.

Library preparation and Illumina sequencing. Previously amplified cDNA libraries were prepared for sequencing using Illumina's TruSeq DNA Sample Preparation Kit. Final library size distribution was determined using Agilent Bioanalyzer 2100 and insert size ranged from 206-246 base pairs (bp). Libraries were pooled and sequenced on two lanes of the Illumina HiSeq2000 platform (San Diego, CA) using the rapid-run mode with 150 bp paired-end reads. The content of each library was divided by half and each half sequenced on one of the two lanes. This was done to avoid lane-related batch effects. A summary of the RNA-Seq data is displayed in Table S2.

Quality control and filtering of sequencing reads. A schematic of the computational pipeline for assembling *C. medius* transcripts from raw sequencing reads, calculating expression levels,

and determining differentially expressed genes between conditions is shown in Figure 3. Quality control processing of the RNA-Seq data was completed using FastQC software developed by Babraham Bioinformatics (Andrews 2010). This software calculates global statistics based on Phred scores and nucleotide composition, including plots of positional Phred scores across the length of all reads, positional nucleotide composition, and relative k-mer enrichment over read length which was used to define parameters for downstream filtering using the software Trimmomatic (Bolger et al. 2014). We removed the Illumina adaptor sequences and trimmed the ends of the reads by checking the first and last three bases and retaining reads with a Phred score >30, with a required minimum length of 100 bp. The median trimmed length for the forward strand was 151 ± 13.34 nucleotides, while the reverse strand had a median trimmed length of 151 ± 9.50 nucleotides.

***De novo* transcriptome assembly.** We constructed a reference *de novo* assembly by pooling the RNA-Seq reads from all samples and using the bioinformatic pipeline Trinity (version: 20130814) (Haas et al. 2013) on a computing cluster with 48 cores and 512Gb RAM. We used the following command line: Trinity.pl --seqType fq --JM 90G --left all_1.fastq --right all_2.fastq --output assembly_output --CPU 22. We obtained 1,295,606 putative transcripts corresponding to 776,170 gene models with an N50 of 981 nucleotides. The number of initially assembled transcripts was very high, due to inclusion of any assembled transcripts longer than 200 nucleotides. Short transcripts are typically discarded downstream. Subsequently, we filtered out putative artifacts, due to polymorphisms and/or sequencing errors, with the program CD-HIT-EST (Fu et al. 2012). By employing a 95% similarity threshold the number of transcripts decreased to 1,206,443. Although the majority or transcripts were quite short (Figure S1) we

were able to reconstruct a large number of long transcripts (225,744 transcripts > 1 Kb). Next, we aligned all the reads to the assembly using Bowtie2 (Langmead & Salzberg 2012) and used the Integrated Genome Viewer (IGV) (Thorvaldsdottir et al. 2013) for data visualization. Finally, we performed sequence similarity searches of the reconstructed transcripts against the human proteome (Ensembl v.73) with BLASTx 2.2.28+ (Camacho et al. 2009). Using an *e*-value < 10^{-4} we found 158,276 transcripts in *C. medius* with a detectable homologous protein in human. After eliminating redundant hits we detected 9,540 transcripts with homology to human proteins (>70% of the protein length). For differential gene expression analysis we used the 15,420 transcripts with homology in humans that expressed in at least 4 samples. Details on the transcript assembly and comparisons to other protocols that were applied to the same dataset can be found in Figure S1, S2 and Table S3.

Investigating the influence of RNA quality on transcriptome assembly. We investigate how RIN scores, which measure RNA integrity, affected the number of assembled transcripts and coverage at the 5'and 3' transcript ends. As expected, the number of reconstructed transcripts was positively correlated with the RIN score of the sample (Figure S2A). However, we also noted that even in samples with very low RIN scores (≤ 5), the number of transcripts recovered was quite large (on average, 67.08% of the number recovered in the best sample).

Using an in-house python script, we clustered together all the reads mapping to each transcript and classified them as 5' if they were located in the first 10% of the transcript, and 3' if they were located in the last 10% of the transcript. When comparing the degree of enrichment or depletion of sequencing reads in either the 5' or 3' regions, we detected a statistically significant

impoverishment in the 3' region in all the samples (one sample Wilcoxon test, mu=0.1). The number of reads in the 3' region was about half the number expected if the reads were homogeneously distributed. Surprisingly, however, we found no correlation between the level of 3' read depletion and the RIN score, suggesting that this bias is intrinsic to the RNA-Seq technique and largely independent of sample quality as indicated by RIN score (Figure S2B).

Identification of human genes expressed in adipose tissue using GTEx data. We downloaded gene expression data for the two RNA-Seq human adipose tissue samples available from the GTEx Consortium (GTEX-N7MS-0326-SM-4E3K2 and GTEX-NFK9-0326-SM-3MJGV (Lonsdale et al. 2013). We determined that 11,875 protein-coding genes were expressed at FPKM > 0.5 in both samples, 8,682 of which corresponded to dwarf lemur assembled genes.

Estimating transcript abundance and differential gene expression. To estimate transcript abundance, we used the software package RSEM (Li & Dewey 2011). We generated a matrix of normalized counts comprised of the number of reads for each sample (columns) mapping to each reconstructed transcript (rows). To identify differentially expressed (DE) transcripts, we used the edgeR Bioconductor package (Robinson et al. 2009). edgeR is based on an over-dispersed Poisson model that accounts for technical and biological variability. We used the following general linear model: ~condition + RIN, to avoid any putative biases created by the range of RIN scores in our samples. We only tested *C. medius* genes with a significant hit against the human proteome (Ensembl v.73) using an *e*-value threshold of 10^{-4}. We discarded any genes in which at least 4 samples had less than 0.5 counts per million (cpm). This was done to remove the effect of poorly supported transcripts in some samples. We identified DE genes for each sample collection

point by analyzing data from three individuals (Tanager, Quetzal, and Osprey; see Table S2). One individual was removed (Towhee) because she lost a significant amount of weight prior to entering torpor, probably as a consequence of the food-restriction guidelines described in the section above, "*Experimental collection points".* Our analyses were performed using pairwise comparisons, as we were focused on detecting differences between physiological states. The individual samples were used to assess the biological variability within each condition.

We corrected p-values for multiple comparisons using the Benjamini-Hochberg method (Benjamini & Hochberg 1995) providing a *p*-value cut-off for significance which controlled the false discovery rate (FDR) at 0.05. We performed a functional annotation clustering analysis of the differentially expressed genes using the Panther Classification System (Panther v.10) (Huaiyu et al. 2016). We interrogated groups of genes that were up- or down-regulated during the Torpor time point in relation to the Active state.

Protein evolutionary rates in hibernating species. We extracted the protein sequence from the Trinity reconstructed transcripts in dwarf lemurs with the best BLASTx match against the human proteome. We selected cases in which we could detect one-to-one orthologous genes in 10 species from Ensembl (v.82), 3 of which are capable of hibernation (marked with an asterisk): *Homo sapiens, Bos taurus, Cavia porcellus, Mus musculus, Myotis lucifugus*, Pteropus vampyrus, Oryctolagus cuniculus, Otolemur garnettii, Spermophilus tridecemlineatus*, and Cheirogaleus medius*.*

We generated multiple sequence alignments with the software Prank+F using the algorithm

PALO for the selection of the most appropriate protein for each gene, instead of the longest one. This methodology has been shown to reduce false positives in the estimation of the rate of non-synonymous to synonymous substitutions (dN/dS = ω) using CodeML (Fletcher and Yang 2010; Villanueva-Cañas et al. 2013). The alignments were manually trimmed afterwards. We compared two different models using CodeML in the PAML package (Yang 2007). The tree with branch distances for CodeML input was modified from Meredith et al. (2011). In the first model, leaves of hibernating species and non-hibernating species were allowed different ω. In the second model all leaves had the same ω value. The likelihood ratio between the two models was obtained with LR = 2*(lnL1-lnL2) with one degree of freedom.

Results

***De novo* transcriptome assembly.** We performed *de novo* transcript assembly using Trinity by concatenating the reads from all twelve collected samples (Tables S1 and S2). Sequence similarity searches with BLASTx revealed that 158,276 transcripts had a detectable homolog in humans. Of these, some of the transcripts were partially reconstructed and were mapped to a redundant human protein. After clustering redundant hits, we annotated 9,540 unique *C. medius* genes with homology to human proteins. A substantial majority of them (8,682; ~91%) were expressed in the two available human GTEx samples from adipose tissue.

Investigating the influence of RNA quality on transcriptome assembly. The preservation of RNA in biological samples is especially challenging in studies performed in the wild, or when samples are problematic to acquire, such as biopsied tissue (Gallego Romero et al. 2014). To investigate the effect of the RIN scores on transcript assembly, we compared the number of

detected transcripts in each sample to the range of RIN values. Although there was some effect across samples, even for samples with very low RIN values, we reconstructed a high number of transcripts with human homologues (Figure S2A). The number of reads falling into 5' and 3' ends of transcripts appeared to be independent of the RIN value (Figure S2B). This suggests that the effects are relatively small. Nevertheless, given that other studies have suggested that this kind of analysis is sensitive to RNA integrity (e.g., Gallego Romero et al. 2014), we explicitly took the RIN values into account when performing the differential gene expression analysis.

Identification of differentially expressed genes. We estimated gene expression levels by mapping back the reads of each individual sample to the dwarf lemur transcript. Subsequently, we performed differential gene expression analysis between pairs of conditions with edgeR. Despite our sampling being longitudinal in nature, we were only interested in comparing each time point in a pair-wise fashion. The linear model employed included the RIN value of the sample. Table 2 shows a summary of the number of differentially expressed genes (FDR < 0.05) uncovered. Only 1 gene was differentially expressed in the Active 1 vs. Active 2 comparison (Table 2). In contrast, more than one hundred genes were differentially expressed in the Active 1 vs. Torpor, and Active 2 vs. Torpor pairwise comparisons, showing an overlap of 71%. This corresponds to 90 differentially expressed genes that consistently change expression patterns during Torpor relative to Active states.

Differentially expressed gene functions and pathways. Functional enrichment analysis was performed with the Panther Classification System after grouping genes both up-regulated and down-regulated during Torpor as distinct groups. This analysis did not show any clear

enrichment in differentially expressed genes after correcting for multiple testing; however, given the manageable number of differentially expressed genes, we examined the function of each gene individually. We highlight genes that show the same pattern of differential expression across all individuals when comparing each physiological state. The complete list of differentially expressed genes for all time point comparisons is provided in Supplementary File 1. Based upon body weight and core T_b data, we do not discriminate between Active 1 and Active 2, but instead treat them as biological replicates to characterize gene expression profiles during an Active physiological state. When comparing Active to Torpor states, we find genes involved in metabolic processes, DNA and protein binding, cellular adhesion, and blood coagulation/circulation to be differentially expressed in a seasonal pattern.

Our experimental design also allowed for investigations into the influence of photoperiod on gene expression profiles. Between Active 1 and Active 2 time points, photoperiod was reduced to simulate the transition from summer to fall. We compared each Active collection point individually to our Torpor collection point. Genes involved in metabolic pathways and fat storage that displayed up-regulation during Torpor include adipose acyl-CoA synthase-1 (*ACSL1*; 2.53-fold over Active 2), aminoadipate-semialdehyde synthase (*AASS*; 4.54-average fold over combined Active 1 and Active 2), pyruvate dehydrogenase kinase 4 (*PDK4*; 1.66-fold over Active 1), and phosphofructokinase platelet (*PFKP*; 3.29-average fold over combined Active 1 and Active 2) (Figure 4).

We also find other genes involved in feeding behavior to have seasonal expression patterns. We find leptin (*LEP*) and its receptor, *LEPR,* to be down-regulated during Torpor when compared to

the Active 1 state (decreased 3.72-fold and 2.31, respectively). Genes implicated in the mammalian circadian clock are also differentially expressed. During Torpor, two isoforms of nuclear factor, interleukin 3 regulated (*NFIL3*), a transcription factor that regulates Period clock genes (*PER1* and *PER2*), are up-regulated 2.57-fold and 2.21-fold over Active 1. *PER1* is up-regulated 1.85-fold over Active 1. Genes involved in the blood coagulation cascade show variable expression patterns throughout the year. When comparing Torpor to the Active 1 state we find that a member of the annexin family (*ANXA4*; 1.80-fold decrease during Torpor) and coagulation factor VIII (*F8*; 2.50-fold decrease) display differential gene expression (Figure 4).

Extreme changes in gene expression across collection points. A number of genes were found to display notable seasonally-dependent changes, as determined by the average log fold change between the combined Active 1 and Active 2 vs. Torpor pairwise comparison. The most drastic examples include desmoplakin (*DSP*; 10.04-fold), membrane bound O-acyltransferase domain containing 2 (*MBOAT2*; 9.23-fold), exophilin 5 (*EXPH5*; 8.09-fold), desmocollin 3 (*DSC3*; 7.58-fold), haptoglobin (*HP*; 7.22-fold), and hydroxysteroid (17-beta) dehydrogenase 6 *(HSD17B6*; 6.29-fold)

Shared genes among mammalian hibernators. Using gene expression profiles generated from our RNA-Seq experiment for the combined Active 1 and Active 2 vs. Torpor pairwise comparison, we used previously published datasets from multiple ground squirrel species, the American black bear, and bats to look at common genes identified as differentially expressed in conjunction with changes in physiology. Table 3 highlights the differentially expressed genes we identify in dwarf lemurs that are also identified as differentially expressed in other hibernating

species.

Protein evolutionary rates. The assembly of a transcriptome *de novo* gave us the opportunity to perform protein sequence comparisons between the dwarf lemur and other species. In particular, we were interested in testing if hibernation-associated genes evolved faster in hibernating species versus in non-hibernating species. We selected a set of 12 genes that had one-to-one orthologues in 9 other mammals, including 2 other hibernating and 7 non-hibernating species (see *Methods* for the list of species). We estimated the rate of non-synonymous versus synonymous substitutions (dN/dS) and compared the likelihood of two models, one in which the dN/dS was independent of the hibernating status and another one in which the dN/dS was assumed to be different between hibernating and non-hibernating species (Figure S3). In only 2 out of 12 cases the second model was more plausible (p-value < 10^{-3}; Supplementary File 2). Although the gene showed a significant increase in dN/dS in the hibernation-associated branches, dN/dS values were nonetheless low (0.057 for *TRPC1* and 0.076 for *S100A1*) and unlikely to reflect positive selection.

Discussion

This study is the first to investigate gene regulation in a hibernating primate, and also the first to longitudinally sample WAT from the same individuals with collection points chosen to correlate with the most drastic changes in physiology throughout the circannual cycle. Thus, our study succeeds in providing novel insights into this remarkable phenotypic phenomenon. The dynamic nature of the dwarf lemur WAT transcriptome provides an expansive view of the molecular mechanisms associated with the physiological changes that allow a hibernating primate to withstand long periods of physical inertia and a total lack of food intake by relying solely upon

stored fat as fuel. Genes involved in metabolic processes, basic cellular processes (e.g. DNA replication and repair, protein trafficking, cell proliferation), cellular adhesion, blood coagulation, and immune response were found to show highly variable expression profiles that correlate with physiological state (Torpor vs. Active). However, we acknowledge that based on lack of significant enrichment from our functional enrichment analysis, our results should be interpreted carefully. Based on our stringent cut-offs in determining differential expression and, therefore, relatively few numbers of differentially expressed genes, we cannot rule out that other genes in the same functional groupings do not show opposite patterns.

Hibernating mammals switch from carbohydrates to lipids as their primary fuel source during the winter hibernation season when seasonal food resources become scarce (Carey et al. 2003; Boyer & Barnes 1999; Buck et al. 2002). Consistent with this physiological transition, we find significant seasonal changes of metabolic gene expression in WAT, including overexpression of fatty acid catabolic genes and lipid transport genes during the winter fasting period. We find instances of other genes involved in fatty acid oxidation that are significantly up-regulated during Torpor relative to the Active state. For example, *ACSL1* belongs to a family of enzymes that catalyze the esterification of fatty acids with CoA. It is suggested that members of the *ACSL* gene family drive the uptake of long-chain fatty acids for β-oxidation, and are required for cold thermogenesis (Ellis et al. 2010). Additionally, *AASS*, a gene product that catalyzes the first two steps in the lysine degradation pathway (Tondo et al. 2013; Sacksteder et al. 2000), is up-regulated during Torpor in dwarf lemur WAT. This is important as a significant amount of metabolic energy can come from amino acid metabolism, especially during starvation conditions, as experienced by hibernating animals. Conversely, we uncover expression profiles of genes

involved in adipogenesis and fatty acid biosynthesis to be significantly down-regulated during Torpor. *ADIRF*, a gene that is thought to be solely expressed in adipose tissue, putatively aids in the activation of transcription factors involved in adipogenesis, and contributes to increased glucose uptake in adipocytes (Ni et al. 2012; Qiu 2013). This gene is overexpressed in human obesity patients (Ni et al. 2012; Qiu 2013), though more functional studies are needed to determine the exact mechanism for its involvement in adipogenesis.

Our study demonstrates that dwarf lemurs show some differentially expressed genes that are also differentially expressed in other hibernating species (Table 3). It is worth noting, however, that differential expression of specific genes or protein products has historically shown little consistency when comparing data from previous studies (Villanueva-Cañas et al. 2014) and indeed, we find opposite patterns in few of the genes we identified in dwarf lemurs as differentially expressed when comparing them to American black bears and bat species. However, a closer look taking physiology into account show that some of these results might not be surprising. *AASS*, involved in lysine degradation, show differences in regulation patterns when comparing dwarf lemur WAT to the liver of two species of ground squirrel. Liver and WAT have different responses to amino acid degradation, so its unsurprising that they would show variable gene expression patterns during a torpor bout in different tissues surveyed. We also find variable regulatory patterns of *PFKP*, a gene involved in glycolysis. Lei et al. (2014) find this gene to be down-regulated in the brain of torpid bats, in contrast to what we find in dwarf lemurs. This can be partly explained by the fact that brain and adipose tissue have unique metabolic profiles, especially during periods of starvation, as in torpid animals. Under starvation conditions, the brain switches from glucose to ketone bodies as fuel, a notion that is supported by

Lei et al's finding. This is not the case in WAT, as glucose conservation may be less important.

These results speak to the challenging nature of studies that examine patterns of comparative gene regulation, as well as the need for consistent sampling strategies. However, it is well established that genes function through pathways. Previous work from our group suggests that by expanding differential gene expression profiles to include genes belonging to the same molecular pathway, a higher proportion of genes are identified as shared between hibernators (e.g. seeing high concordance among datasets in beta-oxidation pathways) (Villanueva-Cañas et al. 2014). This lends support to the hypothesis that hibernating species across mammalian phylogeny have evolved similar approaches of gene regulation to combat periods of resource scarcity, although further investigations are required to fully elucidate this question. In this line, we also tested the hypothesis that hibernation-related genes could be evolving under a model of positive selection in hibernating species in comparison with other mammals. For that we estimated the non-synonymous to synonymous substitution rate ratio (ω) in different branches of a tree containing hibernating and non-hibernating species (Figure S3). We found that the model with significantly higher ω in hibernating species was only supported for 2 out of 12 genes analyzed, which was not significantly different from what would be expected by chance (Supplementary File 2). This is in agreement with previous work wherein we specifically tested the hypothesis that hibernation-related genes were enriched in signals of positive selection (Villanueva-Cañas et al. 2014), finding no support for differential signals of positive selection. Both analyses point in the direction of gene regulation as a key player in the hibernation phenotype rather than the modification of existing genes.

Establishing methodological approaches for investigations with free-ranging populations. Captive conditions offer a unique opportunity for systematically collecting tissue samples under carefully controlled settings. Though the complete longitudinally-sampled group is small (N = 4 individuals), the DLC holds the world's only colony of captive dwarf lemurs, thus providing an exclusive resource for these studies and thus yielding the means to use a sampling approach that has, to our knowledge, not yet been used for transcriptomic-based studies on the hibernation phenotype. The observed duration of torpor bouts and reduction in metabolic rates and T_b are not as extreme in captive animals as those found existing under natural conditions (Dausmann et al. 2005; 2009). Numerous studies in other species have suggested that hibernation patterns differ between intraspecific captive and free-ranging populations (Geiser & Ferguson 2001; Geiser et al. 2007). Although hibernation patterns from captive studies are often used to predict models of energetics and survival in wild populations (Karpovich et al. 2009; Bonaccorso & McNab 1997; Geiser et al. 2007; Bartels et al. 1998; Armitage et al. 2003), the physiology and behavior of hibernation are strongly affected by acclimation to captivity. Nonetheless, captive individuals can be induced to enter bouts of torpor during the winter months through photoperiodic and temperature alterations, with sampling strategies carefully planned for capturing the critical physiological states of interest. Therefore, data from captive studies should be extrapolated to free-ranging populations with caution.

Replicate studies of free-ranging populations in their natural habitat will be crucial for fully understanding the underling genetic mechanisms of primate hibernation. Additionally, leveraging comparative studies of gene expression data from several mammalian hibernators can provide important clues into the specific genetic controls associated with the hibernation

phenotype, in addition to providing insight to questions associated with the evolution of the hibernation phenotype within Class Mammalia.

Ethics statement. Animal handling was carried out in strict accordance with the approval of Duke University's Institutional Animal Care and Use Committee (IACUC protocol #A274-10-10).

Data Accessibility. Raw sequence data were deposited into the NCBI Short Read Archive with accession number SRP049327. Additional data were deposited into Dryad (doi:10.5061/dryad.057b7; reviewer link accessible at http://datadryad.org/review?doi=doi:10.5061/dryad.057b7) and nucleotide alignments for positive selection analysis are uploaded to Figshare (doi: 10.6084/m9.figshare.2013138; reviewer link accessible at https://figshare.com/s/01b4838218146c6187e5).

Acknowledgements. We thank Sandy Martin and Jenny Tung for careful review of the manuscript and appreciate the assistance of the Duke GCB Genome Sequencing Shared Resource staff and DLC staff for making this project possible. This is DLC publication number XXXX.

Funding Statement. This work was supported by grants from the Society of Integrative and Comparative Biology and Sigma Xi to S.L.F., a National Science Foundation Doctoral Research Improvement Grant [NSF-BCS 1455809 to A.D.Y and S.L.F], a grant from the Duke University Institute for Genome Science and Policy to A.D.Y., and funding from the Ministerio de

Economía y Competitividad of the Spanish Government [BIO2009-08160 to J.L.V.C. and BFU2012-36820 to J.L.V.C. and M.M.A.]; and Fundació ICREA to M.M.A.

Authors' contributions. SLF designed the study, performed the laboratory component of the study, generated figures, and led the writing. JLVC optimized and performed the bioinformatics analyses, conducted data analysis, and generated figures. PHK supervised the maintenance of appropriate and consistent captive conditions for initiating torpor. MMA contributed to the design of the bioinformatics pipeline, and ADY supervised and partially funded the project. All authors contributed to the writing and approved the final version of the manuscript.

Competing Interests. The authors declare no competing interests.

References

Andrews S. 2010. FastQC: a quality control tool for high throughput sequence data. http://www.bioinformatics.babraham.ac.uk/projects/fastqc/.

Andrews MT. 2007. Advances in molecular biology of hibernation in mammals. Bioessays. 29:431–440. doi: 10.1002/bies.20560.

Armitage KB, Blumstein DT, Woods BC. 2003. Energetics of hibernating yellow-bellied marmots (Marmota flaviventris). Comparative Biochemistry and Physiology, Part A. 134:101–114.

Bartels W, Law B, Geiser F. 1998. Daily torpor and energetics in a tropical mammal, the northern blossom-bat Macroglossus minimus (Megachiroptera). J Comp Physiol B. 168:233–239.

Bauer VW, Squire TL, Lowe ME, Andrews MT. 2001. Expression of a chimeric retroviral-lipase mRNA confers enhanced lipolysis in a hibernating mammal. Am J Physiol-Reg I. 281:R1186–92.

Benjamini Y, Hochberg Y. 1995. Controlling the False Discovery Rate - a Practical and Powerful Approach to Multiple Testing. Journal of the Royal Statistical Society Series B-Methodological. 57:289–300.

Bolger AM, Lohse M, Usadel B. 2014. Trimmomatic: a flexible trimmer for Illumina sequence data. Bioinformatics. 30:2114–2120. doi: 10.1093/bioinformatics/btu170.

Bonaccorso F, McNab B. 1997. Plasticity of energetics in blossom bats (Pteropodidae): Impact on distribution. J Mammal. 78:1073–1088.

Boyer B, Barnes B. 1999. Molecular and metabolic aspects of mammalian hibernation. Bioscience. 49:713–724.

Boyer B, Barnes B, Lowell B, Grujic D. 1998. Differential regulation of uncoupling protein gene homologues in multiple tissues of hibernating ground squirrels. Am J Physiol. 275:R1232–R1238.

Buck MJ, Squire TL, Andrews MT. 2002. Coordinate expression of the PDK4 gene: a means of regulating fuel selection in a hibernating mammal. Physiological Genomics. 8:5–13. doi: 10.1152/physiolgenomics.00076.2001.

Camacho C et al. 2009. BLAST+. BMC Bioinformatics. 10:421. doi: 10.1186/1471-2105-10-421.

Carey H, Andrews M, Martin S. 2003. Mammalian hibernation: Cellular and molecular responses to depressed metabolism and low temperature. Physiol Rev. 83:1153–1181. doi: 10.1152/physrev.00008.2003.

Chow BA, Donahue SW, Vaughan MR, McConkey B, Vijayan MM. 2013. Serum Immune-Related Proteins are Differentially Expressed during Hibernation in the American Black Bear Xie, L-H, editor. PLoS ONE. 8:e66119. doi: 10.1371/journal.pone.0066119.t003.

Dark J. 2005. Annual lipid cycles in hibernators: Integration of Physiology and Behavior. Annu. Rev. Nutr. 25:469–497. doi: 10.1146/annurev.nutr.25.050304.092514.

Dausmann K, Glos J, Ganzhorn J, Heldmaier G. 2005. Hibernation in the tropics: lessons from a primate. J Comp Physiol B. 175:147–155. doi: 10.1007/s00360-004-0470-0.

Dausmann K, Glos J, Ganzhorn J, Heldmaier G. 2004. Hibernation in a tropical primate. Nature. 429:825–826.

Dausmann KH, Glos J, Heldmaier G. 2009. Energetics of tropical hibernation. J Comp Physiol B. 179:345–357. doi: 10.1007/s00360-008-0318-0.

Demas GE, Bowers RR, Bartness TJ, Gettys TW. 2002. Photoperiodic regulation of gene expression in brown and white adipose tissue of Siberian hamsters (Phodopus sungorus). Am J Physiol-Reg I. 282:R114–21.

Eddy S. 2004. Up-regulation of fatty acid-binding proteins during hibernation in the little brown bat, Myotis lucifugus. Biochimica et Biophysica Acta (BBA) - Gene Structure and Expression. 1676:63–70. doi: 10.1016/j.bbaexp.2003.10.008.

Eddy SF, Morin P, Storey KB. 2005. Cloning and expression of PPAR-gamma and PGC-1alpha from the hibernating ground squirrel, Spermophilus tridecemlineatus. Mol Cell Biochem. 269:175–182.

Eddy SF, Morin P, Storey KB. 2006. Differential expression of selected mitochondrial genes in hibernating little brown bats,Myotis lucifugus. J. Exp. Zool. 305A:620–630. doi: 10.1002/jez.a.294.

Ellis JM et al. 2010. Adipose Acyl-CoA Synthetase-1 Directs Fatty Acids toward β-Oxidation and Is Required for Cold Thermogenesis. Cell Metabolism. 12:53–64. doi: 10.1016/j.cmet.2010.05.012.

Emirbekov EZ, Pashaeva ME. 2014. Expression of cytoskeleton proteins in hypothalamic cells in winter sleeping ground squirrels Citellus pygmaeus Pallas during hibernation. Neurochem. J. 8:178–183. doi: 10.1134/S1819712414020032.

Epperson LE, Martin SL. 2002. Quantitative assessment of ground squirrel mRNA levels in multiple stages of hibernation. Physiological Genomics. 10:93–102. doi: 10.1152/physiolgenomics.00004.2002.

Epperson LE, Rose JC, Carey HV, Martin SL. 2010. Seasonal proteomic changes reveal molecular adaptations to preserve and replenish liver proteins during ground squirrel hibernation. AJP: Regulatory, Integrative and Comparative Physiology. 298:R329–R340. doi: 10.1152/ajpregu.00416.2009.

Faherty SL, Campbell CR, Larsen PA, Yoder AD. 2015. Evaluating whole transcriptome amplification for gene profiling experiments using RNA-Seq. BMC Biotechnol. 1–10. doi: 10.1186/s12896-015-0155-7.

Fedorov VB et al. 2011. Modulation of gene expression in heart and liver of hibernating black bears (Ursus americanus). BMC Genomics. 12:171. doi: 10.1186/1471-2164-12-171.

Fietz J, Dausmann KH. 2007. Big is beautiful: fat storage and hibernation as a strategy to cope with marked seasonality in the fat-tailed dwarf lemur (Cheirogaleus medius). 97–110.

Fietz J, Tataruch F, Dausmann K, Ganzhorn J. 2003. White adipose tissue composition in the free-ranging fat-tailed dwarf lemur (Cheirogaleus medius; Primates), a tropical hibernator. J Comp Physiol B. 173:1–10. doi: 10.1007/s00360-002-0300-1.

Fletcher W, Yang Z. 2010. The effect of insertions, deletions, and alignment errors on the branch-site test of positive selection. Mol Biol Evol 27:2257–2267. doi:10.1093/molbev/msq115.

Fu L, Niu B, Zhu Z, Wu S, Li W. 2012. CD-HIT: accelerated for clustering the next-generation sequencing data. Bioinformatics. 28:3150–3152. doi: 10.1093/bioinformatics/bts565.

Gallego Romero,I, Pail AA, Tung J, Gilad Y. 2014. RNA-seq: impact of RNA degradation on transcript quantification. BMC Biology. 12:42 doi:10.1186/1741-7007-12-42

Geiser F, Ferguson C. 2001. Intraspecific differences in behaviour and physiology: effects of captive breeding on patterns of torpor in feathertail gliders. J Comp Physiol B. 171:569–576. doi: 10.1007/s003600100207.

Geiser F, Heldmaier G. 1995. The impact of dietary fats, photoperiod, temperature and season on morphological variables, torpor patterns, and brown adipose tissue fatty acid composition of hamsters, Phodopus sungorus. J. Comp. Physiol. B, Biochem. Syst. Environ. Physiol. 165:406–415.

Geiser F, Holloway JC, Körtner G. 2007. Thermal biology, torpor and behaviour in sugar gliders: a laboratory-field comparison. J Comp Physiol B. 177:495–501. doi: 10.1007/s00360-007-0147-6.

Grabek KR, Diniz Behn C, Barsh GS, Hesselberth JR, Martin SL. 2015. Enhanced stability and polyadenylation of select mRNAs support rapid thermogenesis in the brown fat of a hibernator. eLife. 4. doi: 10.7554/eLife.04517.022.

Haas BJ et al. 2013. De novo transcript sequence reconstruction from RNA-seq using the Trinity platform for reference generation and analysis. Nature Protocols. 8:1494–1512. doi: 10.1038/nprot.2013.084.

Hampton M et al. 2011. Deep Sequencing the Transcriptome Reveals Seasonal Adaptive Mechanisms in a Hibernating Mammal Gimble, JM, editor. PLoS ONE. 6:e27021. doi: 10.1371/journal.pone.0027021.t006.

Hampton M, Melvin RG, Andrews MT. 2013. Transcriptomic Analysis of Brown Adipose Tissue across the Physiological Extremes of Natural Hibernation Dahlman-Wright, K, editor. PLoS ONE. 8:e85157. doi: 10.1371/journal.pone.0085157.s002.

Herminghuysen D, Vaughan M, Pace RM, Bagby G, Cook CB. 1995. Measurement and seasonal variations of black bear adipose lipoprotein lipase activity. Physiol Behav. 57:271–275.

Huaiyu M, Poudel S, Muruganujan A, Casagrande JT, Thomas PD. 2016. PANTHER version 10: expanded protein families and functions, and analysis tools. Nucl. Acids Res. doi: 10.1093/nar/gkv1194

Kabine M et al. 2004. Peroxisome proliferator-activated receptors as regulators of lipid metabolism; tissue differential expression in adipose tissues during cold acclimatization and hibernation of jerboa. Biochimie. 86:763–770. doi: 10.1016/j.biochi.2004.10.003.

Karpovich SA, Tøien Ø, Buck CL, Barnes BM. 2009. Energetics of arousal episodes in hibernating arctic ground squirrels. J Comp Physiol B. 179:691–700. doi: 10.1007/s00360-009-0350-8.

Krystal AD et al. 2013. The Relationship of Sleep with Temperature and Metabolic Rate in a Hibernating Primate. PLoS ONE. 8:e69914. doi: 10.1371/journal.pone.0069914.t001.

Langmead B, Salzberg SL. 2012. Fast gapped-read alignment with Bowtie 2. Nat Meth. 9:357–359. doi: 10.1038/nmeth.1923.

Lei M, Dong D, Mu S, Pan Y-H, Zhang S. 2014. Comparison of Brain Transcriptome of the Greater Horseshoe Bats (Rhinolophus ferrumequinum) in Active and Torpid Episodes. PLoS ONE. 9:e107746. doi: 10.1371/journal.pone.0107746.s004.

Li B, Dewey CN. 2011. RSEM: accurate transcript quantification from RNA-Seq data with or without a reference. BMC Bioinformatics. 12:323. doi: 10.1186/1471-2105-12-323.

Lonsdale J et al. 2013. The Genotype-Tissue Expression (GTEx) project. Nat. Genet. 45:580–585. doi: 10.1038/ng.2653.

Lovegrove BG, Lobban KD, Levesque DL. 2014. Mammal survival at the Cretaceous-Palaeogene boundary: metabolic homeostasis in prolonged tropical hibernation in tenrecs. Proc Roy Soc B. 281, 20141304–20141304. doi: 10.1098/rspb.2011.0190.

Meredith RW, Janečka JE, Gatesy J, et al. 2011. Impacts of the Cretaceous Terrestrial Revolution and KPg extinction on mammal diversification. Science 334:521–524. DOI: 10.1126/science.1211028

Mominoki K. 1998. Haptoglobin in the brown bear (Ursus arctos): Molecular structure and hibernation-related seasonal variations. Japenese Journal of Veterinary Research. 46:100–101.

Mominoki K et al. 2005. Elevated plasma concentrations of haptoglobin in European brown bears during hibernation. Comparative Biochemistry and Physiology-Part A: Molecular &

Integrative Physiology. 142:472–477. doi: 10.1016/j.cbpa.2005.09.017.

Morin P, Storey KB. 2009. Mammalian hibernation: differential gene expression and novel application of epigenetic controls. Int. J. Dev. Biol. 53:433–442. doi: 10.1387/ijdb.082643pm.

Ni Y et al. 2012. A Novel pro-adipogenesis factor abundant in adipose tissues and over-expressed in obesity acts upstream of PPARγ and C/EBPα. J Bioenerg Biomembr. 45:219–228. doi: 10.1007/s10863-012-9492-6.

Nowak J, Mzilikazi N, Dausmann KH. 2013. Torpor as an emergency solution in Galago moholi: heterothermy is triggered by different constraints. J Comp Physiol B. 183(4):547-556

Ortmann S, Heldmaier G, Schmid J, Ganzhorn JU. 1997. Spontaneous daily torpor in Malagasy mouse lemurs. *Naturwissenschaften* **84,** 28–32.

Perret M, Aujard F. 2001. Daily hypothermia and torpor in a tropical primate: synchronization by 24-h light-dark cycle. Am J Physiol-Reg I. 281:R1925–33.

Perret M, Aujard F, Vannier G. 1998. Influence of daylength on metabolic rate and daily water loss in the male prosimian primate Microcebus murinus. Comparative Biochemistry and Physiology-Part A: Molecular & Integrative Physiology. 119:981–989.

Qiu J. 2013. Overexpression of C10orf116 promotes proliferation, inhibits apoptosis and enhances glucose transport in 3T3-L1 adipocytes. Mol Med Report. doi: 10.3892/mmr.2013.1351.

Reis dos M et al. 2012. Phylogenomic datasets provide both precision and accuracy in estimating the timescale of placental mammal phylogeny. Proceedings of the Royal Society B: Biological Sciences. 279:3491–3500. doi: 10.1073/pnas.122231299.

Robinson MD, McCarthy DJ, Smyth GK. 2009. edgeR: a Bioconductor package for differential expression analysis of digital gene expression data. Bioinformatics. 26:139–140. doi: 10.1093/bioinformatics/btp616.

Ruf T, Streicher U, Stalder GL, Nadler T, Walzer C. 2015. Hibernation in the pygmy slow loris (Nycticebus pygmaeus): Multiday torpor in primates is not restricted to Madagascar. Sci Rep. 5:17392. doi: 10.1038/srep17392

Ruiz-Orera J, Messeguer X, Subirana JA, Albà MM. 2014. Long non-coding RNAs as a source of new peptides. eLife. 3. doi: 10.7554/eLife.03523.027.

Sacksteder KA et al. 2000. Identification of the α-aminoadipic semialdehyde synthase gene, which is defective in familial hyperlysinemia. The American Journal of Human Genetics. 66:1736–1743.

Schmid J. 2001 Daily torpor in free-ranging gray mouse lemurs (Microcebus murinus) in Madagascar. Int J Primatol. 22(6): 1021-1031.

Schwartz C, Hampton M, Andrews MT. 2013. Seasonal and Regional Differences in Gene Expression in the Brain of a Hibernating Mammal. PLoS ONE. 8:e58427. doi: 10.1371/journal.pone.0058427.s003.

Seim I et al. 2013. Genome analysis reveals insights into physiology and longevity of the Brandt's bat Myotis brandtii. Nature Communications. 4:1–8. doi: 10.1038/ncomms3212.

Shao C et al. 2010. Shotgun Proteomics Analysis of Hibernating Arctic Ground Squirrels. Molecular & Cellular Proteomics. 9:313–326. doi: 10.1074/mcp.M900260-MCP200.

Srere H, Wang L, Martin S. 1992. Central role for differential gene expression in mammalian hibernation. P Natl Acad Sci USA. 89:7119–7123.

Sun L et al. 2013. Long noncoding RNAs regulate adipogenesis. P Natl Acad Sci USA. 110:3387–3392. doi: 10.1073/pnas.1222643110.

Suozzi A, Malatesta M, Zancanaro C. 2009. Subcellular distribution of key enzymes of lipid metabolism during the euthermia-hibernation-arousal cycle. Journal of Anatomy. 214:956–962. doi: 10.1111/j.1469-7580.2009.01086.x.

Thorvaldsdottir H, Robinson JT, Mesirov JP. 2013. Integrative Genomics Viewer (IGV): high-performance genomics data visualization and exploration. Briefings in Bioinformatics. 14:178–192. doi: 10.1093/bib/bbs017.

Toien O et al. 2011. Hibernation in Black Bears: Independence of Metabolic Suppression from Body Temperature. Science. 331:906–909. doi: 10.1126/science.1199435.

Tondo M et al. 2013. Clinical, biochemical, molecular and therapeutic aspects of 2 new cases of 2-aminoadipic semialdehyde synthase deficiency. Molecular Genetics and Metabolism. 110:231–236. doi: 10.1016/j.ymgme.2013.06.021.

Vermillion KL, Anderson KJ, Hampton M, Andrews MT. 2015. Gene expression changes controlling distinct adaptations in the heart and skeletal muscle of a hibernating mammal. Physiological Genomics. doi: 10.1152/physiolgenomics.00108.2014.

Villanueva-Cañas JL, Faherty SL, Yoder AD, Albà MM. 2014. Comparative Genomics of Mammalian Hibernators Using Gene Networks. Integrative and Comparative Biology. doi: 10.1093/icb/icu048.

Villanueva-Cañas JL, Laurie S, Albà MM. 2013. Improving genome-wide scans of positive selection by using protein isoforms of similar length. Genome Biol Evol. 5(2): 457-467. doi: 10.1093/gbe/evt017.

Williams DR. 2005. Seasonally hibernating phenotype assessed through transcript screening. Physiological Genomics. 24:13–22. doi: 10.1152/physiolgenomics.00301.2004.

Wilson BE, Deeb S, Florant GL. 1992. Seasonal changes in hormone-sensitive and lipoprotein lipase mRNA concentrations in marmot white adipose tissue. Am J Physiol. 262:R177–81.

Yan J. 2006. Detection of differential gene expression in brown adipose tissue of hibernating arctic ground squirrels with mouse microarrays. Physiological Genomics. 25:346–353. doi: 10.1152/physiolgenomics.00260.2005.

Yang Z. 2007. PAML 4: Phylogenetic Analysis by Maximum Likelihood. Mol Biol Evol 24 (8): 1586-1591.doi: 10.1093/molbev/msm088

Figure Legends

Fig. 1. The patchwork distribution of heterothermic species within the mammalian phylogeny demonstrates that hibernation is likely a retained ancestral trait. Orange box denotes Monotremata, yellow box indicates Marsupialia, and green box defines Placentalia. Families colored in blue text indicate the inclusion of at least one species that is heterothermic. Representative heterothermic species are pictured on right. No distinction was made between summer heterothermy and winter heterothermy. Phylogeny modified from dos Reis et al. 2012.

Fig. 2. Schematic representation of timeline for experimental design. Solid black line indicates cyclic body weight changes during the year. Dotted red line depicts ambient temperatures used during study period. Circles along the x-axis indicate photoperiodic changes that occurred during the study period, mimicking the switch from autumn to winter day lengths.

Fig. 3. Overview of the bioinformatics pipeline used in this study

Fig. 4. Boxplot graph showing significant expression (BH <0.05) changes between physiological states for highlighted genes mentioned in the text. Y axis shows the number of reads in log10 scale that map to each reconstructed gene, while boxplot whiskers show the range of reads between individuals.

Figure 1.

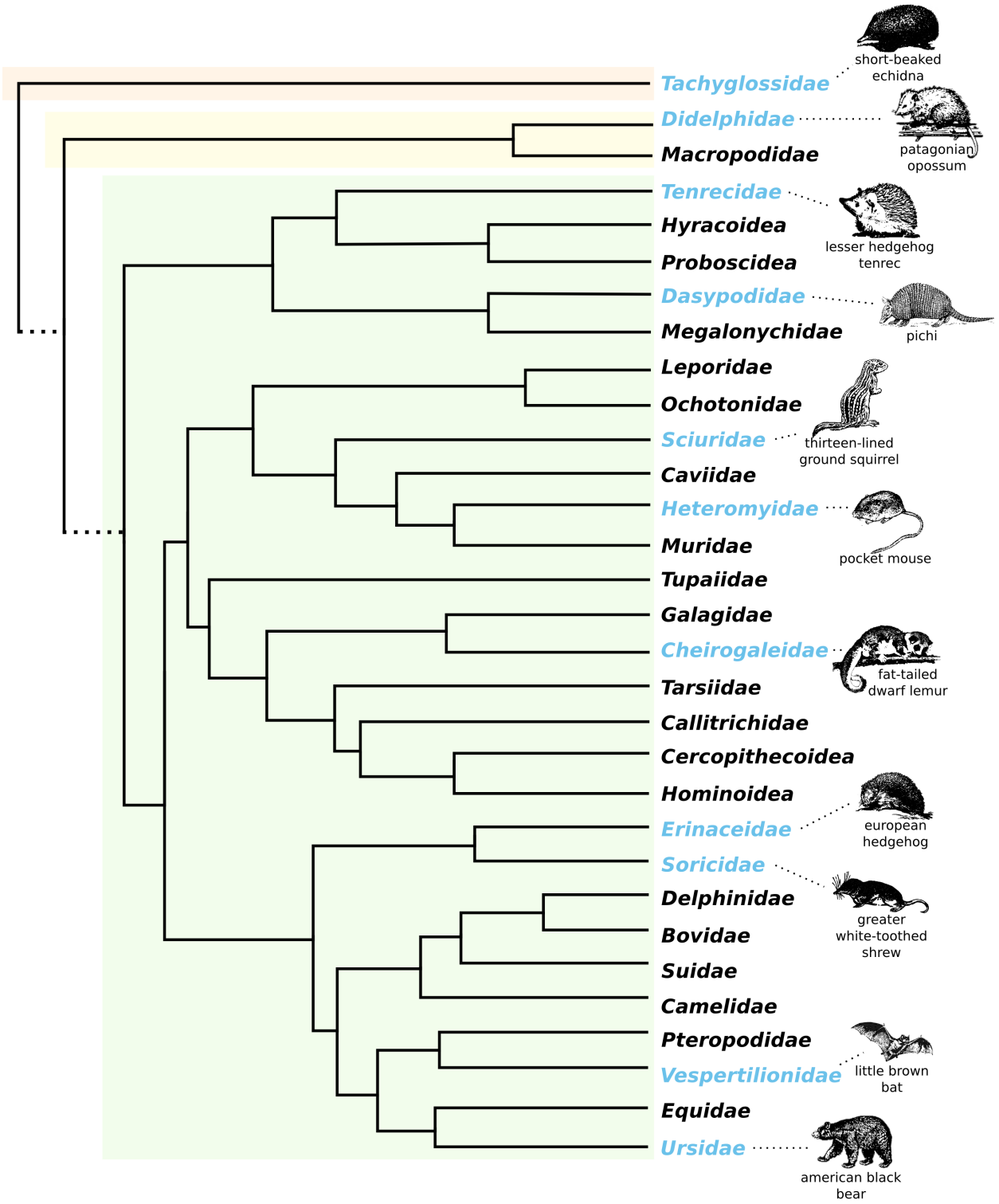

Figure 2.

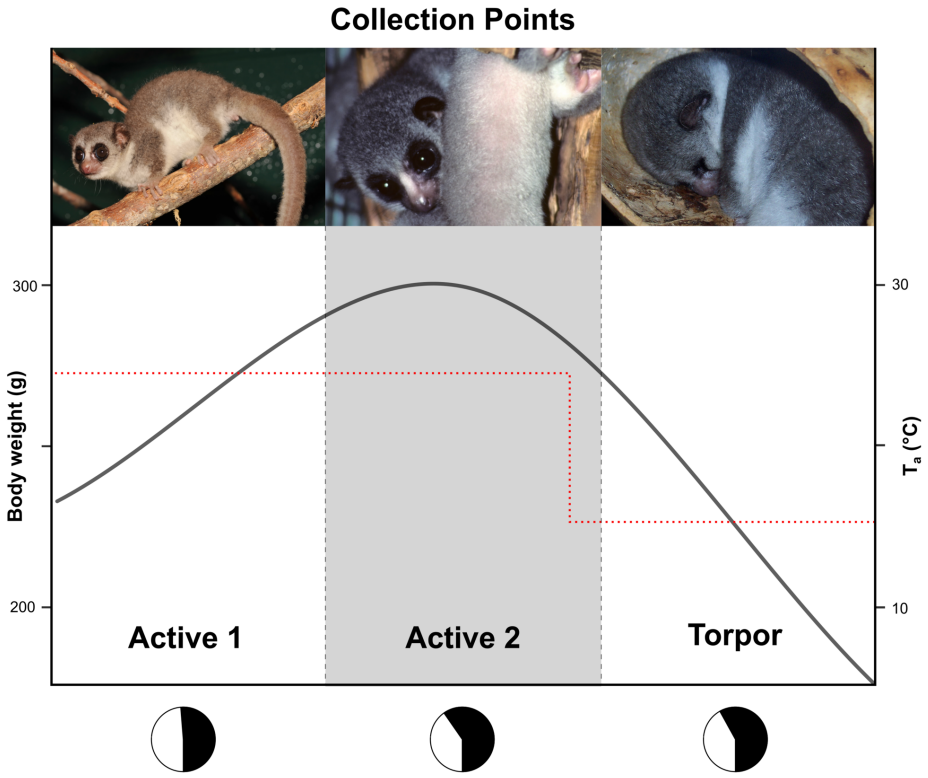

Figure 3.

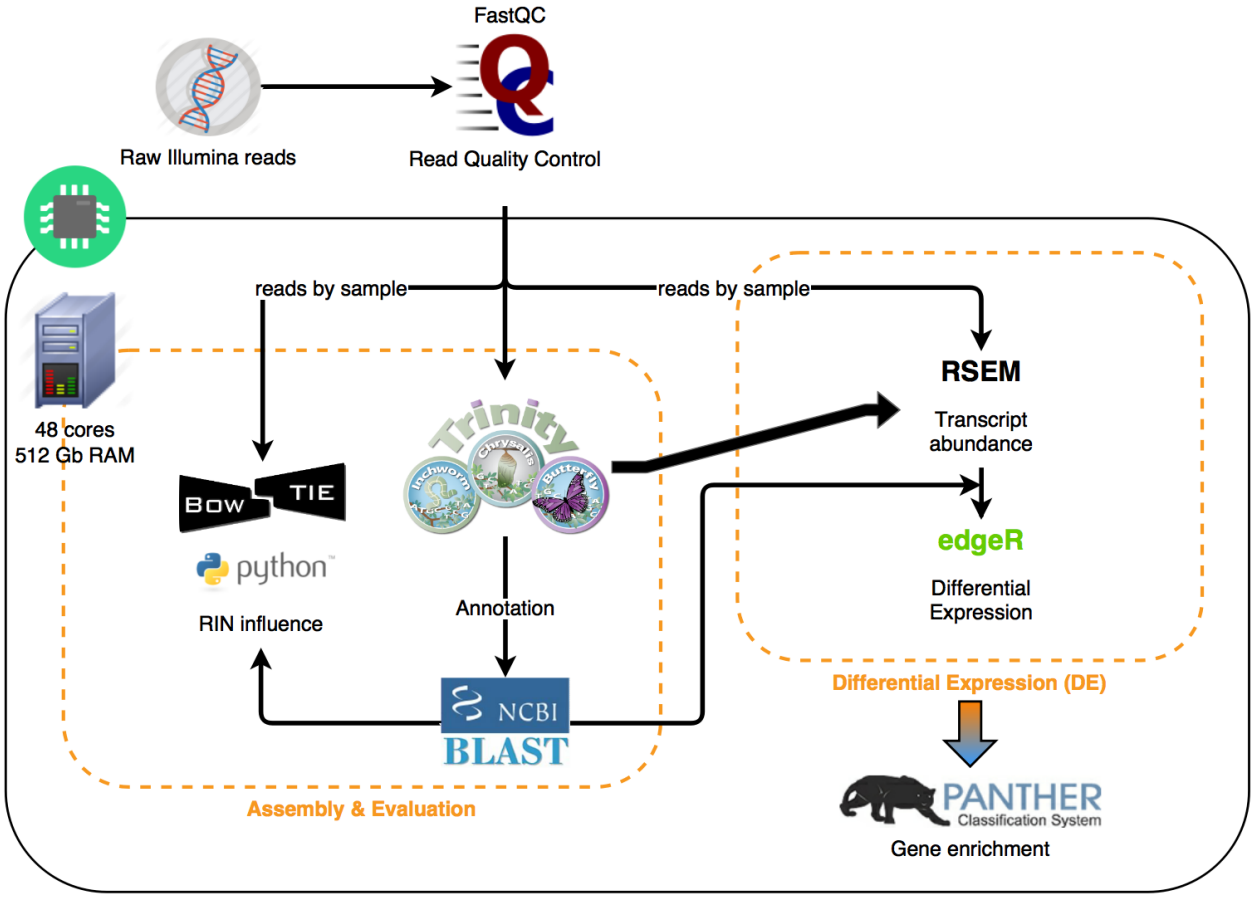

Figure 4.

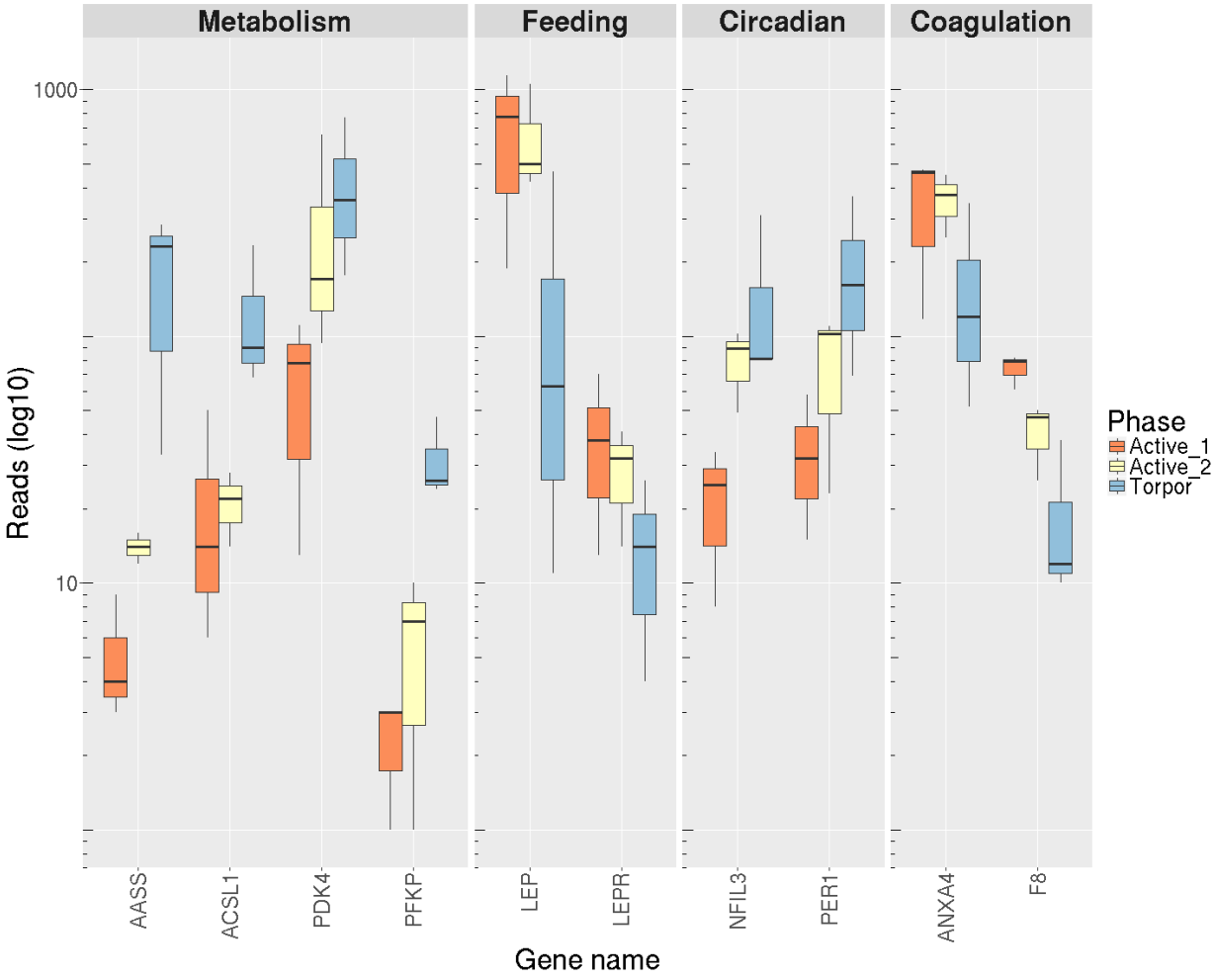

Table 1. Collection points and corresponding states of activity, mean body mass (±SD), mean body temperature (rectal T_b; ±SD), ambient temperature (T_a), and photoperiod during sample collection.

Collection Point	Physiological state	Body mass (g)	T_b (°C)	T_a (°C)	Photoperiod
October 2012	Active 1	238.7 ± 32.1	33.9 ± 0.1	25	LD 11.5:12.5
December 2012	Active 2	237.3 ± 29.3	35.3 ± 1.8	25	LD 9.5:14.5
February 2013	Torpor	196.0 ± 57.2	19.8 ± 4.1	15	LD 10.5:13.5

Table 2. Total number of genes assessed for differential expression and differentially expressed genes (DE) among different physiological conditions.

Pairwise Comparison	DE genes with sequence similarity to human *(e-value < 10^{-4})*
Active 1 vs. Torpor	283
Active 2 vs. Torpor	126
Active 1 + Active 2 vs. Torpor	90
Active 1 vs. Active 2	1

Table 3. Differentially expressed genes in Active 1 + Active 2 vs. Torpor collection point with homolog in another hibernating species determined from previous studies

Gene Name	Symbol	logFC	References
Metabolism and metabolic processes			
aminoadipate-semialdehyde synthase	*AASS*	5.02	Shao *et al*., 2010; Epperson *et al*., 2010
Phosphofructokinase, platelet	*PFKP*	3.66	Lei *et al*., 2014
Basic cellular processes			
inhibitor of DNA binding 4	*ID4*	-2.42	Schwartz *et al*., 2013
phosphodiesterase 1A, calmodulin-dependent	*PDE1A*	-3.30	Schwartz *et al*., 2013
pleckstrin homology-like domain, family B, member 2	*PHLDB2*	-1.48	Fedorov *et al*., 2012
S100 calcium binding protein A1	*S100A1*	-2.22	Emiberkov and Pashaeva, 2014; Schwartz *et al*., 2013; Vermillion *et al*. 2015
Circulation and blood coagulation			
Haptoglobin	*HP*	7.06	Mominoki 1998; Mominoki *et al*., 2005; Yan *et al*., 2008; Chow *et al*., 2013; Vermillion *et al*. 2015